nature communications

Article

https://doi.org/10.1038/s41467-024-50897-7

Deoxygenative radical cross-coupling of $C(sp^3)$–O/$C(sp^3)$–H bonds promoted by hydrogen-bond interaction

Received: 1 April 2024

Accepted: 24 July 2024

Published online: 08 August 2024

Check for updates

Yue Wang[1,2], Suping Zhang[2,3], Ke Zeng[2], Pengli Zhang[2], Xiaorong Song[2], Tie-Gen Chen[1,2] ✉ & Guoqin Xia[1,2] ✉

Building $C(sp^3)$-rich architectures using simple and readily available starting materials will greatly advance modern drug discovery. $C(sp^3)$–H and $C(sp^3)$–O bonds are commonly used to strategically disassemble and construct bioactive compounds, respectively. However, the direct cross coupling of these two chemical bonds to form $C(sp^3)$–$C(sp^3)$ bonds is rarely explored in existing literature. Conventional methods for forming $C(sp^3)$–$C(sp^3)$ bonds via radical-radical coupling pathways often suffer from poor selectivity, severely limiting their practicality in synthetic applications. In this study, we present a single electron transfer (SET) strategy that enables the cleavage of amine α-C − H bonds and heterobenzylic C − O bonds to form $C(sp^3)$–$C(sp^3)$ bonds. Preliminary mechanistic studies reveal a hydrogen bond interaction between substrates and phosphoric acid facilitates the cross-coupling of two radicals with high chemoselectivity. This methodology provides an effective approach to a variety of aza-heterocyclic unnatural amino acids and bioactive molecules.

One of the fundamental tasks in synthetic organic chemistry is to create structurally and functionally diverse architectures from simple and abundant feedstocks. C–H and C–O bonds are among the most commonly utilized chemical bonds for strategically disconnecting and constructing complex molecules[1–4]. However, the direct cross-coupling of the C–O bond and C–H bond to form the $C(sp^3)$–$C(sp^3)$ bond has remained a challenging and unexplored area[5] (Fig. 1a). Over the past century, the transition metal-catalyzed C–C bond forming reactions have garnered immense interest from both the academic and industrial communities. Although traditional transition metal-catalyzed cross-coupling reactions, such as the Suzuki reaction developed in the 1960s, have achieved significant success in synthetic practices, they still lack broad applicability in constructing $C(sp^3)$–$C(sp^3)$ bonds due to β-hydride elimination side reaction[6,7]. Recent advances in nickel-catalyzed single electron transfer processes could partially address this limitation, by forming a high-valent Ni(III) reactive intermediate[8–19]. Another approach to forging the $C(sp^3)$–$C(sp^3)$ bond is through the radical addition reactions to the activated double or triple bonds, which typically require precise matching of the substrate electronic properties. Nevertheless, conventional radical–radical direct coupling reactions often lack chemoselectivity between two radicals that are similar in electronic properties, leading to the formation of complex by-products (Fig. 1b). In light of these limitations, we questioned if sp^3-hybridized C–O and C–H bond could be disassembled and rearranged to forge $C(sp^3)$–$C(sp^3)$ bond in a chemo-selective way through the process of photoredox catalysis while maintaining compatibility with various aza-heterocyclic frameworks.

Owing to the development of various directing groups, transition metal-catalyzed C–H bond activation reactions have now emerged as a powerful toolbox in organic synthesis[20–23]. In recent years, the combination of photoredox catalysis and transition metal catalysis has propelled this field towards the exploration of non-directed substrates[24,25]. The remarkable works from Macmillan's group demonstrated a series of elegant photoredox-nickel dual catalytic processes for constructing $C(sp^3)$–$C(sp^2)$ and $C(sp^3)$–$C(sp^3)$ bonds

[1]School of Pharmaceutical Sciences, Southern Medical University, Guangzhou 510515, China. [2]Zhongshan Institute for Drug Discovery, Shanghai Institute of Materia Medica, Chinese Academy of Sciences, Zhongshan, China. [3]Guangzhou University of Chinese Medicine, Guangzhou 510006, China.
✉e-mail: chentiegen@simm.ac.cn; xiaguoqin@simm.ac.cn

https://doi.org/10.1038/s41467-024-50897-7

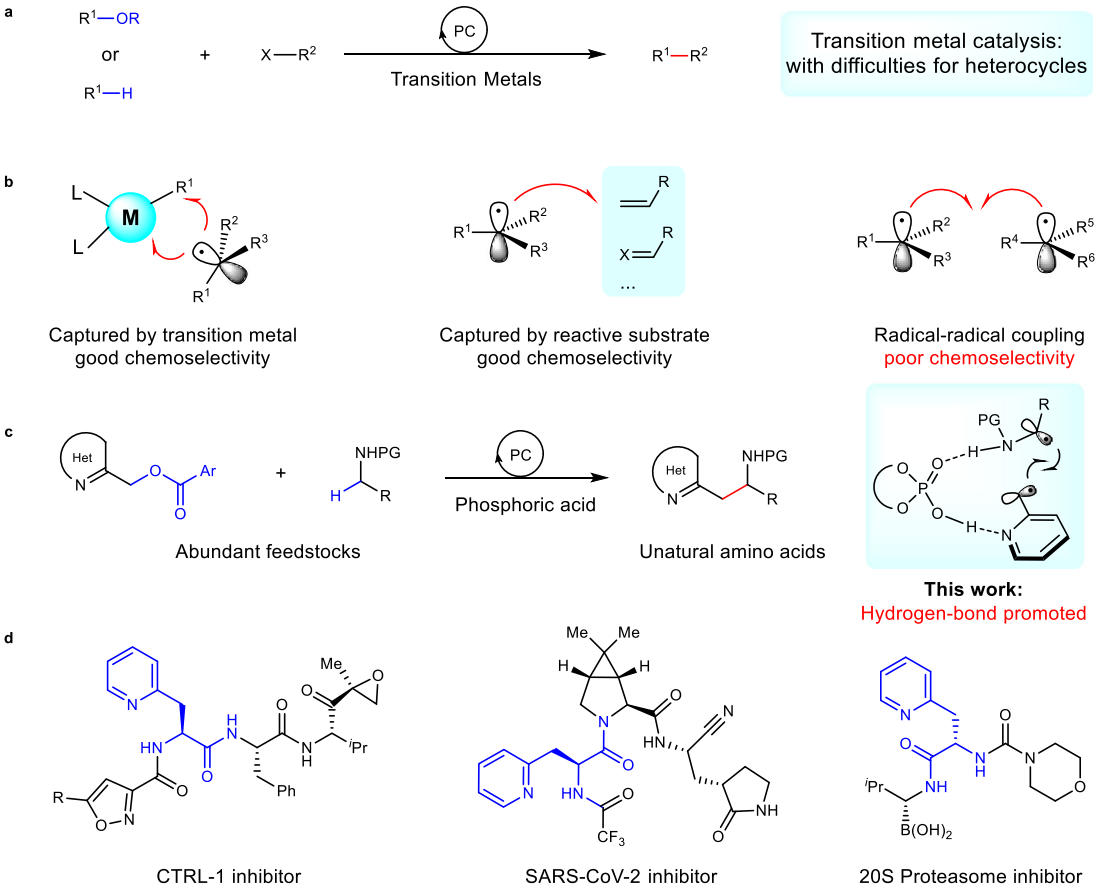

Fig. 1 | Hydrogen-bond interaction promoted radical-radical cross-coupling. **a** Photo-induced transition metal-catalyzed cross-coupling of C–O or C–H bond with C–X bond. **b** Representative radical reaction paradigms. **c** Chemoselective radical cross-coupling of heterobenzylic C–O bond with C–H bond. **d** Aza-heterocyclic unnatural amino acid moieties in bioactive molecules.

from C–H bonds[26–28]. These reactions typically involve the cleavage of C–H bonds at the α-position of amine or alcohol substrates using a HAT reagent. This is then followed by a cross-coupling reaction with aryl halides or alkyl halides, catalyzed by nickel species. It has been reported that the α-C–H bond on glycine derivatives can also serve as an imine precursor under certain oxidation conditions[29–36]. This imine intermediate can then be captured by a variety of nucleophiles or radicals. However, it should be noted that these C–C bond-forming reactions generally require the presence of transition metals and are not compatible with aza-heterocyclic motifs in some cases. In a similar vein, the classic cleavage of C–O bonds involves oxidative addition reactions to generate reactive organometallic intermediates, which are catalyzed by transition metals[37]. This is typically observed for sp^2 hybridized C–O bonds. Alternatively, $C(sp^3)$–$C(sp^3)$ bond cross-coupling reactions can also be conducted for sp^3 hybridized C–O bonds, employing tosylates or triflates as the reactants[38–41]. Recently, it has been reported that the C–O bond can also generate a carbon-centered radical through the use of an acyl-activating reagent or a carbene catalyst[42–47]. Subsequently, this radical is transferred onto the transition metal species and results in the formation of a high valent organometallic intermediate, enabling the formation of a $C(sp^3)$–$C(sp^3)$ bond through a reductive elimination pathway.

In contrast to the abundant availability of alcohols and amines as organic feedstocks, it is intriguing that there have been limited reports on their direct coupling reactions. To address this challenge, we proposed an approach that merges photocatalysis with intermolecular hydrogen bond interactions to enable a redox-neutral and chemoselective radical cross-coupling protocol. Our hypothesis is that the heterobenzylic alcohol can be activated by an electron-deficient benzoyl group, leading to the generation of a free radical upon accepting a single electron from the photocatalyst, as previously reported[42,43]. Simultaneously, the lone pair electrons in the amine substrate can also provide an electron under photocatalytic conditions. Thus, these two substrates create an electron donor–acceptor system, resulting in the formation of two free radicals. These radicals can then undergo a radical–radical cross-coupling reaction facilitated by hydrogen bond interactions (Fig. 1c). This approach will hold great promise for the synthesis of heterocyclic unnatural amino acids, which are commonly found in natural products and bioactive compounds (Fig. 1d).

Results

We opted for 2-hydroxymethylpyridine as the electron acceptor and glycine derivatives as the electron donor for our preliminary investigation. Firstly, the 2-hydroxymethylpyridine was esterified using 3,5-bis(trifluoromethyl)benzoic chloride, while the glycine derivative was converted into a methyl ester.

We were thrilled to discover that pyridin-2-ylmethyl-3,5-bis(trifluoromethyl)benzoate (**1a**) and N-phenylmethyl glycinate (**2a**) were successfully activated by the photocatalyst $Ir(ppy)_3$, and the resulting radicals underwent cross-coupling with a 49% yield. This initial finding prompted us to further investigate the aryl groups on the glycinate substrate. The presence of strong electron-withdrawing groups, such as the trifluoromethyl group on the benzene ring, was found to have a negative impact on the reaction. On the other hand, electron-donating groups like methoxy led to a slightly lower yield, while a fluoride atom in the para-position displayed the highest yield (Table 1, entry 1–4). Furthermore, we tested a range of alcohol-activating acyl groups under

https://doi.org/10.1038/s41467-024-50897-7

Table 1 | Optimization of reaction conditions[a]

Entry	Derivation standard conditions	Yield (%)[b]
1	Ar = 3,5-di-CF_3-C_6H_3 (**1a**), R = Ph (**2a**)	49
2	Ar = **1a**, R = 4-CF_3-C_6H_4 (**2b**)	8
3	Ar = **1a**, R = 4-F-C_6H_4 (**2c**)	53
4	Ar = **1a**, R = 4-OMe-C_6H_4 (**2d**)	32
5	Ar = 2,4,6-trifluorobenzene (**1b**), R = **2a**	37
6	Ar = 2,4,6-trichlorobenzene (**1c**), R = **2a**	15
7	Ar = 4-CF_3-C_6H_4 (**1d**), R = **2a**	40
8	Ar = **1a**, R = **2a**, DME as solvent	33
9	Ar = **1a**, R = **2a**, MeCN as solvent	33
10	Ar = **1a**, R = **2a**, without PA	40
11	Ar = **1a**, R = **2c**, $NaHCO_3$ (2 eq)	64
12	Ar = **1a**, R = **2c**, $NaHCO_3$ (2 eq), 60 °C	72
13	the same conditions as entry 12, in DME	74
14	the same conditions as entry 12, without Ir	19
15	the same conditions as entry 12, in the dark	0

[a]Performed with alcohol **1a** (0.2 mmol, 2.0 equiv), amine **2a** (0.1 mmol, 1.0 equiv), in 1.0 mL of CH_2Cl_2, 24 h. [b]Yields were determined by isolation. PA: 1,1-Binaphthyl-2,2-diyl hydrogenphosphate.

the photoredox conditions. It was determined that 3,5-bis(trifluoromethyl)benzoate (**1a**) was the most effective single electron accepting group for this deoxygenative cross-coupling, with other benzoates showing comparatively lower yields or no coupling product at all in the case of electron-donating benzoates (Table 1, entry 5–7). Solvents were also evaluated, and the results revealed that dichloromethane performed the best compared to the others (Table 1, entry 8–9). Control experiments were also conducted, and the results demonstrated a decrease in yield without the involvement of phosphoric acid (Table 1, entry 10). The yield was improved to 64% when 2.0 equivalents of sodium bicarbonate were added, which was further improved to 72% at 60 °C. The solvent 1,2-Dimethoxyethane could slightly improve the yield to 74% (Table 1, entry 11–13). Furthermore, the reaction produced a yield of 19% in the absence of the iridium catalyst, indicating that these two substrates may form a weak electron-donor-acceptor (EDA) complex under the reaction conditions (Table 1, entry 14). Lastly, no product was observed when the reaction was conducted in the dark, indicating that light emission was essential to the single electron transfer process (Table 1, entry 15).

With the optimal conditions in hand, we embarked on an exploration of the range of substrates for this reaction (Fig. 2 and Fig. 3). Firstly, we reexamined N-(para-methoxyphenyl) (PMP) substituted glycinate using the optimum conditions, resulting in a yield of 67% (**1**). This is of great significance for the practicality of this protocol, as the PMP group is readily removed under oxidation conditions. Subsequently, we examined the substitution of groups with varying electronic properties and positions on the pyridine ring. The results indicated that electron-donating groups, such as methoxy (**3**), as well as electron-withdrawing groups like fluoride and bromide (**4, 5**), provided moderate yields for the 3-substituted pyridines. Similar results were obtained for the 4-substituted pyridines, with no notable impact of the electronic properties of the substituents on the reaction efficiency (**6**–**9**). Likewise, the 5-substituted pyridines offered moderate to good yields without any apparent electronic effect (**10**–**16**). We also investigated substitution groups at the 6-position of the pyridine, and the results revealed an intriguing steric effect on this reaction. The yield decreased as the atomic radius increased from fluoride to bromide (**17**–**19**). This phenomenon suggests that hydrogen bond interactions play a crucial role in the success of this reaction, as steric bulky groups are not conducive to its formation. Multi-substituted pyridines also yielded satisfactory results with moderate to good yields (**22**–**24**). It is worth noting that all the halogen atoms were compatible in this reaction, allowing for further modification of the coupling product. Additionally, the substrates derived from 4-pyridin-methanol and 3-pyridin-methanol exhibited yields of 51% and 72%, respectively (**25, 26**). Considering the challenges encountered in synthesizing unnatural amino acids containing nitrogen heterocycles using traditional methods, we decided to shift our focus towards exploring alternative aza-heterocyclic substrates. To our delight, a range of aza-heterocycles performed well under the reaction conditions. The substrate derived from 2-pyrimidine methanol achieved a yield of 63% (**27**), other aza-heterocycles such as isoquinoline (**28**), oxazole (**29**), thiazole (**30, 31**), imidazole (**32, 34**), and pyrazole (**33**) all exhibited moderate yields. Furthermore, a series of secondary alcohol derivatives were tested under optimal conditions, resulting in moderate to good yields, albeit without significant diastereoselectivity (**35**–**40**). This approach also demonstrated remarkable capability in forming quaternary all-carbon centers through cross-coupling reactions between tertiary alcohols and glycine derivatives(**41**–**46**), which are typically a significant challenge in transition-metal-catalyzed cross-coupling reactions.

Having demonstrated a broad scope for the heterobenzylic alcohol substrates, our interest turned to expand the scope of potential coupling partners (Fig. 4). A series of α-amino ketones were found to work well under the reaction conditions. For instance, α-aminoacetophenone yielded 71% (**47**), while both electron-donating and electron-withdrawing substituents on the benzene ring resulted in moderate to good yields (**47**–**52**). Furthermore, various heteroaromatic amino ketones also exhibited good to moderate yields in this reaction (**53**-**56**). Aliphatic amino ketones were tested as well, all of which provided good yields (**57**–**59**). Notably, benzyl amine only proved effective in this reaction when an electron-withdrawing group was present on the benzene ring, resulting in a moderate yield (**60**). To showcase the versatility of this method in constructing complex

https://doi.org/10.1038/s41467-024-50897-7

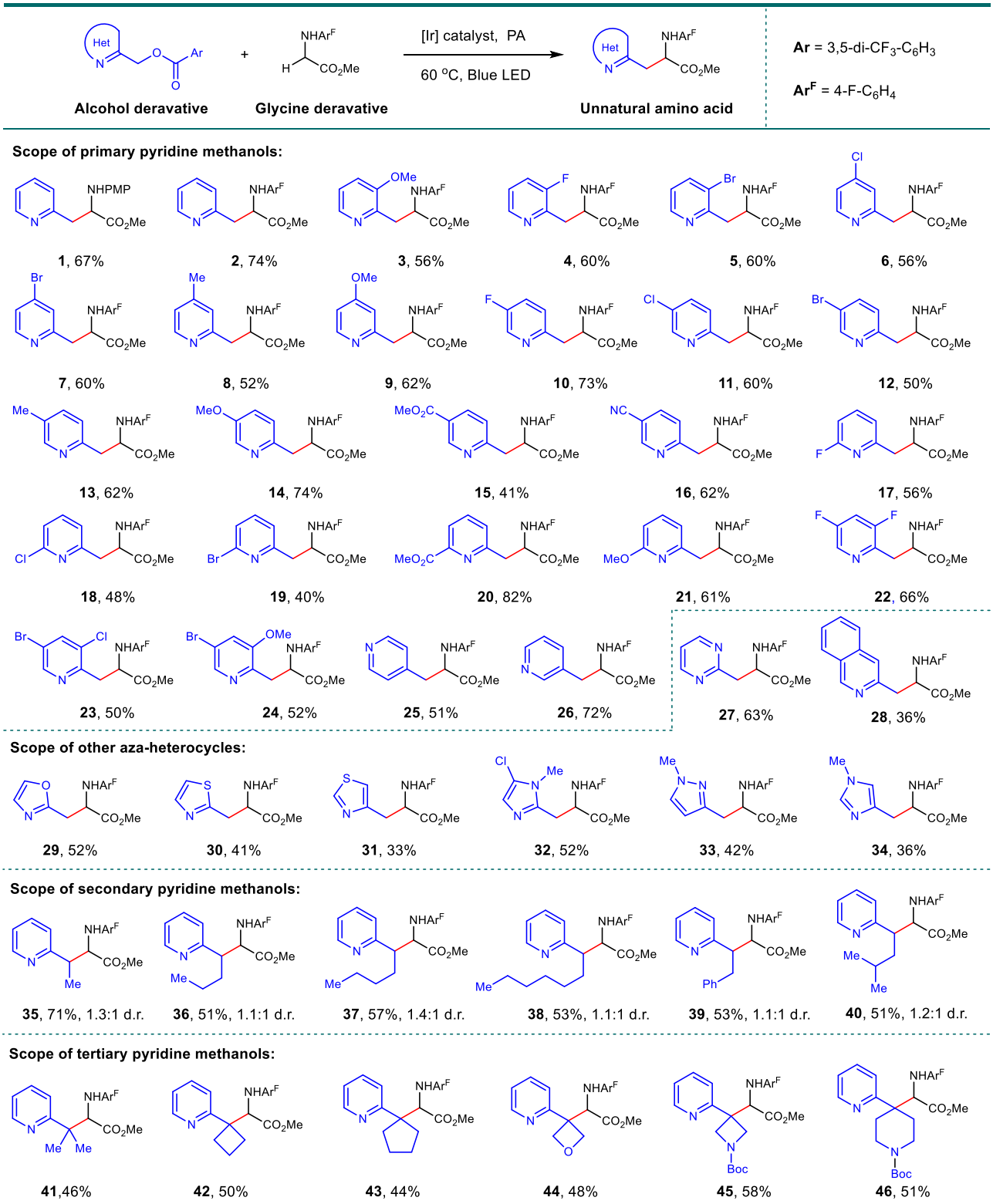

Fig. 2 | Substrate investigation for the heterobenzylic alcohols. All of the yields were isolated yields. The diastereomeric ratio was determined by isolation yield.

functional molecules, we examined a series of peptides containing glycine residues. To our delight, all of these substrates, including dipeptides and tripeptides, performed well and yielded good to excellent results (**61**–**64**). Additionally, we attached a range of chiral auxiliaries to the glycine substrates in order to explore the stereoselective potential of this reaction. Ultimately, we discovered that chiral 2,5-diphenyl pyrrolidine exhibited the best diastereoselectivity (**65**–**69**). Furthermore, this method proved to be highly convenient for the late-stage modification of the beta-adrenergic receptor blocker Pirifibrate (**71**) and the synthesis of histone deacetylase inhibitor (**74**)[48].

To gain further insight into the mechanism underlying this coupling reaction, a series of control experiments were conducted. Initially, when benzylic alcohol was used as the substrate, no product was observed (Fig. 4a). This observation suggests that the presence of a

https://doi.org/10.1038/s41467-024-50897-7

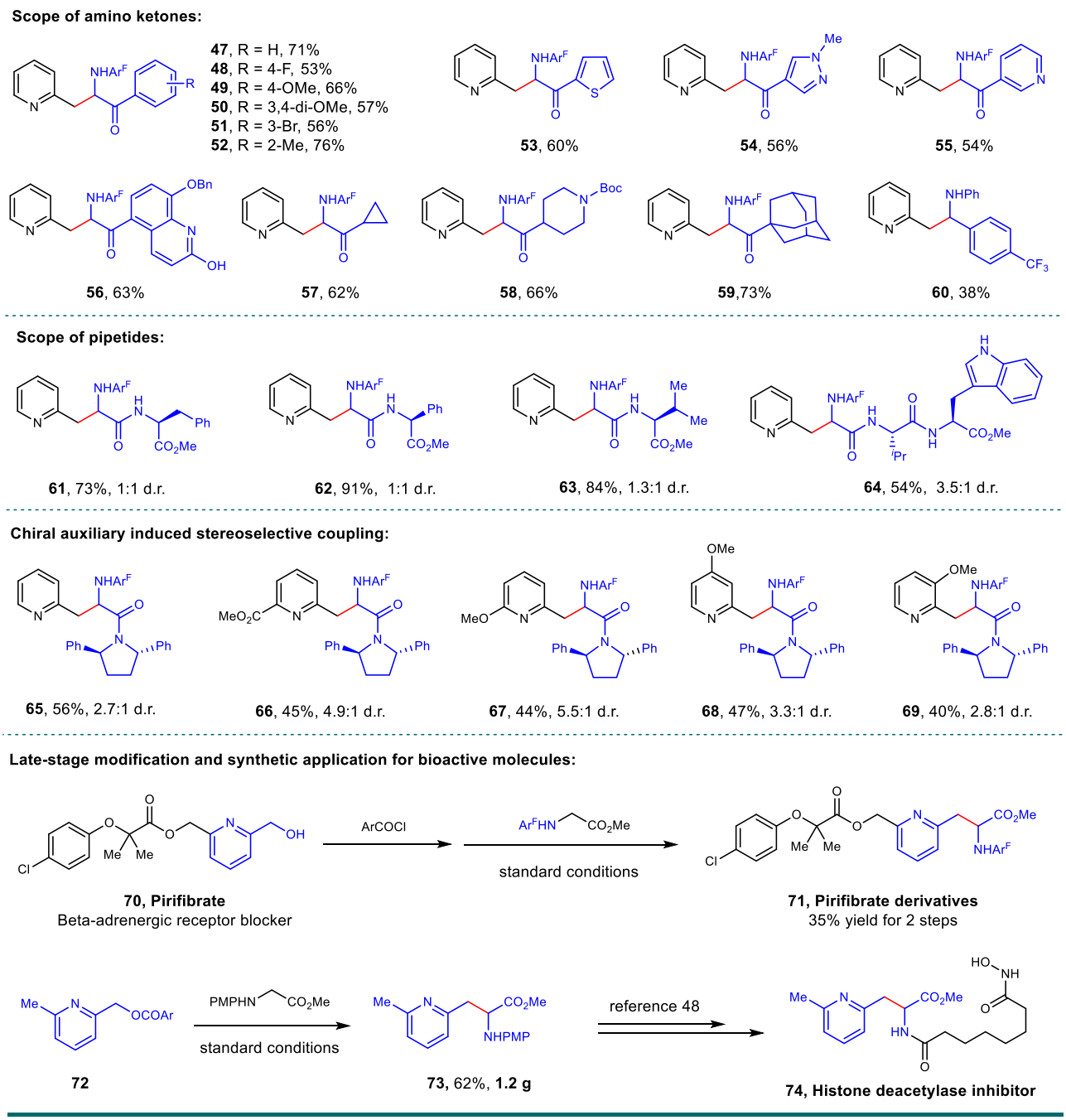

Fig. 3 | Substrate investigation for the amines and synthetic applications. All of the yields were isolated yields. The diastereomeric ratio was determined by isolation yield.

nitrogen atom on the substrate is essential for the success of the reaction. We speculate that the nitrogen atom not only stabilizes the newly formed radical but also provides a lone pair electron for hydrogen bond interaction. Additionally, control experiments showed that the yield decreased significantly from 72% to 38% for 2-pyridine methanol substrate (**1a**) in the absence of phosphoric acid, this result was particularly obvious for 3-pyridine methanol substrate (**26**) which decreased from 72% to 19% yield without the participation of phosphoric acid. In contrast, no obvious decrease in the yield for the 4-pyridine methanol substrate without the phosphoric acid, indicating the reactivity of this substrate was mainly controlled by polarity-matching of two radicals (Fig. 4b). Furthermore, the ^{1}H NMR tracking experiments also revealed that the chemical shifts for both substrates and phosphoric acid protons changed significantly when these compounds were mixed together (see Supplementary Fig. 3 and Supplementary Fig. 4). These observations indicated that phosphoric acid did promote the radical-radical cross-coupling via hydrogen bond interaction along with the polarity-matching of two radicals in this reaction. An effort was also made to capture the radical intermediate by adding TEMPO to the reaction conditions. The heterobenzylic alcohol was converted into the TEMPO-trapped product **75** with a yield of 10% (Fig. 4c), indicating the formation of a pyridyl methylene radical in the reaction. Furthermore, Minisci-type side product **76** and homo-coupling product **77** were also isolated in yields of 5% and 8%, respectively (Fig. 4d), suggesting that the glycine substrate also underwent a radical process. In order to explore the potential

https://doi.org/10.1038/s41467-024-50897-7

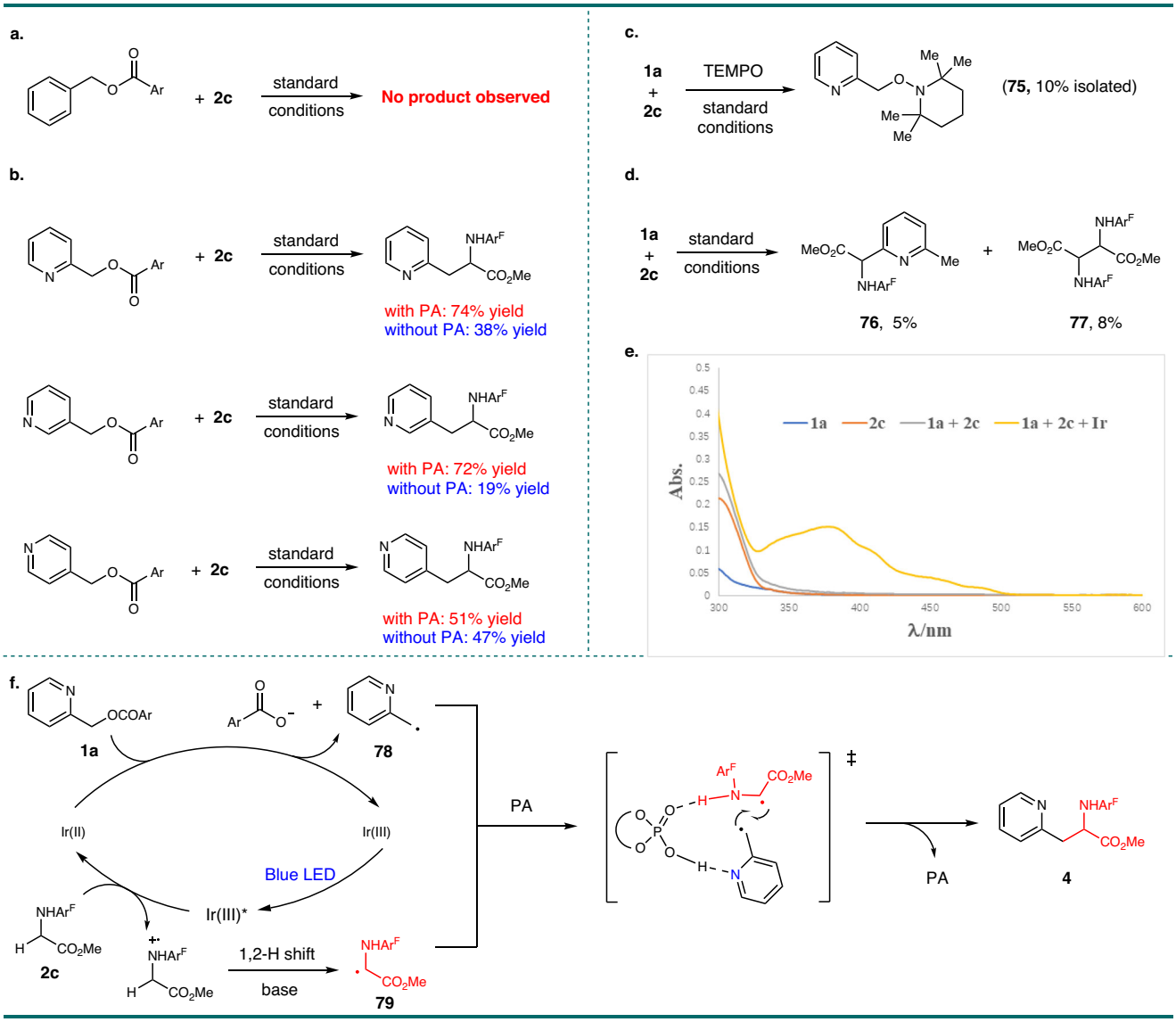

Fig. 4 | Mechanistic insight into the reaction. a Control experiment using benzylic alcohol as substrate. **b** Control experiments in the absence of phosphoric acid. **c** Radical-trapping experiment. **d** Product distribution of the reaction. **e** Optical absorption spectra for the reaction components. **f** Proposed reaction pathways.

formation of an electron-donor-acceptor (EDA) complex in this reaction[49–51], we conducted optical absorption spectra tests on substrates **1a, 2c**, and their combination. The results revealed that the combination of **1a** and **2c** did not display a significant red shift (Fig. 4e), indicating that the EDA complex is not strong enough to effectively drive this reaction. Therefore, we propose that the single electron transfer (SET) process in this reaction occurs through the utilization of an iridium photocatalyst as the mediator for electron transfer. Based on these findings, we have put forward a proposed reaction pathway illustrated in Fig. 4f. Substrate **1a** accepts one electron from the reductive iridium species, leading to the formation of a pyridyl methylene radical intermediate (**78**). Concurrently, substrate **2c** donates one electron to the oxidative iridium species, resulting in a radical at the α-position of the amine (**79**). The cross-coupling of **78** with **79**, facilitated by hydrogen bond interaction with phosphoric acid, ultimately results in the formation of the $C(sp^3)$–$C(sp^3)$ bond.

Discussion

In summary, we have presented an approach for the direct deoxygenative $C(sp^3)$–$C(sp^3)$ cross-coupling of heterobenzylic alcohols and amine substrates. This protocol demonstrates a wide range of substrate compatibility and shows good tolerance towards various functional groups, resulting in moderate to high yields of the desired products. A diastereoselective version of this reaction was also achieved by using a chiral 2,5-diphenyl pyrrolidine as the chiral auxiliary. Importantly, this approach offers a convenient route to access a variety of heterocyclic unnatural amino acids, which are highly valuable in the fields of drug discovery and chemical biology research. Preliminary mechanistic investigations suggest that this reaction proceeds through a radical-radical cross-coupling pathway facilitated by hydrogen bond interactions. This methodology is expected to find broad applications in the efficient synthesis of challenging sp^3-riched heterocyclic unnatural amino acid scaffolds.

Methods

General procedure for the deoxygenative cross-coupling of $C(sp^3)$–O/$C(sp^3)$–H bonds

Substrate **1a** (0.20 mmol), **2c** (0.10 mmol), iridium photocatalyst (0.002 mmol), phosphoric acid (0.03 mmol), sodium bicarbonate (0.20 mmol), and anhydrous 1,2-Dimethoxyethane (1.0 ml) were added sequentially to a 5 ml sealed tube with a magnetic stir bar. The tube was then flushed with N_2 gas for 15 s and sealed with Teflon cap

immediately. The reaction mixture was irradiated under a blue LED ($\lambda = 450$ nm) at 60 °C for 24 h. The mixture was cooled to room temperature, diluted with 2 ml of ethyl acetate, and washed with saturated $NaHCO_3$ solution; the aqueous phase was extracted with ethyl acetate (2 ml) 2 times. The organic phase was combined, dried with anhydrous sodium sulfate, and concentrated. The residue was purified by preparative thin-layer chromatography to provide the cross-coupling product with a 74% yield. Full experimental details and characterization of compounds are given in the Supplementary Information.

Data availability

The data supporting the findings of this study are available within the article and its Supplementary Information files. All other data supporting the findings of this study are available within the Article and its Supplementary Information, or from the corresponding author upon request.

References

1. Ertl, P. & Schuhmann, T. A systematic cheminformatics analysis of functional groups occurring in natural products. *J. Nat. Prod.* **82**, 1258–1263 (2019).
2. Dalton, T., Faber, T. & Glorius, F. C–H activation: toward sustainability and applications. *ACS Cent. Sci.* **7**, 245–261 (2021).
3. Lam, N. Y. S., Wu, K. & Yu, J.-Q. Advancing the logic of chemical synthesis: C–H activation as strategic and tactical disconnections for C–C bond construction. *Angew. Chem. Int. Ed.* **133**, 15901–15924 (2021).
4. Boit, T. B., Bulger, A. S., Dander, J. E. & Garg, N. K. Activation of C–O and C–N bonds using non-precious metal catalysis. *ACS Catal.* **10**, 12109–12126 (2020).
5. Choi, J. & Fu, G. C. Transition metal-catalyzed alkyl-alkyl bond formation: another dimension in cross-coupling chemistry. *Science* **356**, No. eaaf7230 (2017).
6. Jana, R., Pathak, T. P. & Sigman, M. S. Advances in transition metal (Pd, Ni, Fe)-catalyzed cross-coupling reactions using alkyl-organometallics as reaction partners. *Chem. Rev.* **111**, 1417–1492 (2011).
7. Johansson Seechurn, C. C. C., Kitching, M. O., Colacot, T. J. & Snieckus, V. Palladium-catalyzed cross-coupling: a historical contextual perspective to the 2010 Nobel prize. *Angew. Chem. Int. Ed.* **51**, 5062–5085 (2012).
8. Zhou, J. & Fu, G. C. Cross-couplings of unactivated secondary alkyl halides: room-temperature nickel-catalyzed Negishi reactions of alkyl bromides and iodides. *J. Am. Chem. Soc.* **125**, 14726–14727 (2003).
9. Wang, Z., Yin, H. & Fu, G. C. Catalytic enantioconvergent coupling of secondary and tertiary electrophiles with olefins. *Nature* **563**, 379–383 (2018).
10. Huo, H., Gorsline, B. J. & Fu, G. C. Catalyst-controlled doubly enantioconvergent coupling of racemic alkyl nucleophiles and electrophiles. *Science* **367**, 559–564 (2020).
11. Giovannini, R., Stüdemann, T., Dussin, G. & Knochel, P. An efficient nickel-catalyzed cross-coupling between sp^3 carbon centers. *Angew. Chem. Int. Ed.* **37**, 2387–2390 (1998).
12. Gao, Y., Zhang, B., He, J. & Baran, P. S. Ni-electrocatalytic enantioselective doubly decarboxylative C(sp^3)–C(sp^3) cross coupling. *J. Am. Chem. Soc.* **145**, 11518–11523 (2023).
13. Zhang, B. et al. Complex molecule synthesis by electrocatalytic decarboxylative cross-coupling. *Nature* **623**, 745–751 (2023).
14. Zhang, B. et al. Ni-electrocatalytic C(sp^3)–C(sp^3) doubly decarboxylative coupling. *Nature* **606**, 313–318 (2022).
15. Kang, K. & Weix, D. J. Nickel-catalyzed C(sp^3)–C(sp^3) cross-electrophile coupling of in situ generated NHP esters with unactivated alkyl bromides. *Org. Lett.* **24**, 2853–2857 (2022).
16. Sun, D. & Doyle, A. G. Ni/Photoredox-catalyzed C(sp^3)–C(sp^3) coupling between aziridines and acetals as alcohol-derived alkyl radical precursors. *J. Am. Chem. Soc.* **144**, 20067–20077 (2022).
17. Hao, Y. et al. Nickel-catalyzed enantioconvergent reductive hydroalkylation of unactivated alkenes with α-pyridyl alkyl electrophiles. *ACS Catal.* **13**, 15633–15640 (2023).
18. Chen, M. & Montgomery, J. Nickel-catalyzed intermolecular enantioselective heteroaromatic C–H alkylation. *ACS Catal.* **12**, 11015–11023 (2022).
19. Canivet, J., Yamaguchi, J., Ban, I. & Itami, K. Nickel-catalyzed biaryl coupling of heteroarenes and aryl halides/triflates. *Org. Lett.* **11**, 1733–1736 (2009).
20. He, J., Wasa, M., Chan, K. S. L., Shao, Q. & Yu, J.-Q. Palladium-catalyzed transformations of alkyl C–H bonds. *Chem. Rev.* **117**, 8754–8786 (2017).
21. Gandeepan, P. & Ackermann, L. Transient directing groups for transformative C–H activation by synergistic metal catalysis. *Chem* **4**, 199–222 (2018).
22. Sambiagio, C. et al. A comprehensive overview of directing groups applied in metal-catalyzed C–H functionalization chemistry. *Chem. Soc. Rev.* **47**, 6603–6743 (2018).
23. Rej, S., Ano, Y. & Chatani, N. An efficient tool in C–H bond functionalization chemistry for the expedient construction of C–C bonds. *Chem. Rev.* **120**, 1788–1887 (2020). Bidentate Directing Groups.
24. Chan, A. Y. et al. Metallaphotoredox: the merger of photoredox and transition metal catalysis. *Chem. Rev.* **122**, 1485–1542 (2022).
25. Twilton, J. et al. The merger of transition metal and photocatalysis. *Nat. Rev. Chem.* **1**, 0052 (2017).
26. Shaw, M. H., Shurtleff, V. W., Terrett, J. A., Cuthbertson, J. D. & MacMillan, D. W. C. Native functionality in triple catalytic cross-coupling: sp^3 C–H bonds as latent nucleophiles. *Science* **352**, 1304–1308 (2016).
27. Le, C., Liang, Y., Evans, R. W., Li, X. & MacMillan, D. W. C. Selective sp^3 C–H alkylation via polarity-match-based cross-coupling. *Nature* **547**, 79–83 (2017).
28. Perry, I. B. et al. Direct arylation of strong aliphatic C–H bonds. *Nature* **560**, 70–75 (2018).
29. Che, C., Lu, Y.-N. & Wang, C.-J. Enantio- and diastereoselective De Novo synthesis of 3-substituted proline derivatives via cooperative photoredox/Brønsted acid catalysis and epimerization. *J. Am. Chem. Soc.* **145**, 2779–2786 (2023).
30. Che, C., Li, Y.-N., Cheng, X., Lu, Y.-N. & Wang, C.-J. Visible-light-enabled enantioconvergent synthesis of α-amino acid derivatives via synergistic Brønsted acid/photoredox catalysis. *Angew. Chem. Int. Ed.* **60**, 4698–4704 (2021).
31. Yang, L. et al. Molecular oxygen-mediated radical alkylation of C(sp^3)–H bonds with boronic acids. *Org. Lett.* **23**, 3207–3210 (2021).
32. Wang, Z.-H. et al. TEMPO-enabled electrochemical enantioselective oxidative coupling of secondary acyclic amines with ketones. *J. Am. Chem. Soc.* **143**, 15599–15605 (2021).
33. Salman, M., Zhu, Z.-Q. & Huang, Z.-Z. Dehydrogenative cross-coupling reaction between N-aryl α-amino acid esters and phenols or phenol derivative for synthesis of α-aryl α-amino acid esters. *Org. Lett.* **18**, 1526–1529 (2016).
34. Gao, X.-W. et al. Visible light catalysis assisted site-specific functionalization of amino acid derivatives by C–H bond activation without oxidant: cross-coupling hydrogen evolution reaction. *ACS Catal.* **5**, 2391–2396 (2015).
35. Zhang, G., Zhang, Y. & Wang, R. Catalytic asymmetric activation of a C(sp^3)–H bond adjacent to a nitrogen atom: a versatile approach to optically active α-alkyl α-amino acids and C1-alkylated tetrahydroisoquinoline derivatives. *Angew. Chem. Int. Ed.* **50**, 10429–10432 (2011).

36. Zhao, L. & Li, C.-J. Functionalizing glycine derivatives by direct C–C bond formation. *Angew. Chem. Int. Ed.* **47**, 7075–7078 (2008).
37. Qiu, Z. & Li, C.-J. Transformations of less-activated phenols and phenol derivatives via C–O cleavage. *Chem. Rev.* **120**, 10454–10515 (2020).
38. Komeyama, K., Michiyuki, T. & Osaka, I. Nickel/Cobalt-catalyzed C(sp^3)–C(sp^3) cross-coupling of alkyl halides with alkyl tosylates. *ACS Catal.* **9**, 9285–9291 (2019).
39. Liu, J.-H. et al. Copper-catalyzed reductive cross-coupling of non-activated alkyl tosylates and mesylates with alkyl and aryl bromides. *Chemistry* **20**, 15334–15338 (2014).
40. Greene, M. A., Yonova, I. M., Williams, F. J. & Jarvo, E. R. Traceless directing group for stereospecific nickel-catalyzed alkyl-alkyl cross-coupling reactions. *Org. Lett.* **14**, 4293–4296 (2012).
41. Wisniewska, H. M., Swift, E. C. & Jarvo, E. R. Functional-group-tolerant, nickel-catalyzed cross-coupling reaction for enantioselective construction of tertiary methyl-bearing stereocenters. *J. Am. Chem. Soc.* **135**, 9083–9090 (2013).
42. Chen, H.-W. et al. Asymmetric deoxygenative cyanation of benzyl alcohols enabled by synergistic photoredox and copper catalysis. *Chin. J. Chem.* **38**, 1671–1675 (2020).
43. Lu, F.-D. et al. Asymmetric propargylic radical cyanation enabled by dual organophotoredox and copper catalysis. *J. Am. Chem. Soc.* **141**, 6167–6172 (2019).
44. Sakai, A. & MacMillan, D. W. C. Nontraditional fragment couplings of alcohols and carboxylic acids: C(sp^3)–C(sp^3) cross-coupling via radical sorting. *J. Am. Chem. Soc.* **144**, 6185–6192 (2022).
45. Dong, Z. & MacMillan, D. W. C. Metallaphotoredox-enabled deoxygenative arylation of alcohols. *Nature* **598**, 451–456 (2021).
46. Lyon, W. L. & MacMillan, D. W. C. Expedient access to under-explored chemical space: deoxygenative C(sp^3)–C(sp^3) cross-coupling. *J. Am. Chem. Soc.* **145**, 7736–7742 (2023).
47. Intermaggio, N. E., Millet, A., Davis, D. L. & MacMillan, D. W. C. Deoxytrifluoromethylation of alcohols. *J. Am. Chem. Soc.* **144**, 11961–11968 (2022).
48. Schäfer, S. et al. Pyridylalanine-containing hydroxamic acids as selective HDAC6 inhibitors. *ChemMedChem* **4**, 283–290 (2009).
49. Mulliken, R. S. Molecular compounds and their spectra. III. The interaction of electron donors and acceptors. *J. Phys. Chem.* **56**, 801–822 (1952).
50. Rosokha, S. V. & Kochi, J. K. Fresh look at electron-transfer mechanisms via the donor/acceptor bindings in the critical encounter complex. *Acc. Chem. Res.* **41**, 641–653 (2008).
51. de Lima, C. G. S. M., Lima, T., Duarte, M., Jurberg, I. D. & Paixão, M. W. Organic synthesis enabled by light-irradiation of EDA complexes: theoretical background and synthetic applications. *ACS Catal.* **6**, 1389–1407 (2016).

Acknowledgements

We gratefully acknowledge the 100 Talents Program of the Chinese Academy of Sciences, the National Natural Science Foundation of China (22271297), and the Program for Young Talented Investigators of Guangdong Province (2021QN020533) for their financial support. Correspondence and requests for materials should be addressed to G. X. (xiaguoqin@simm.ac.cn).

Author contributions

G. X. and Y. W. conceived the concept and developed the radical cross-coupling of the C(sp^3)–O and C(sp^3)–H bond. Y. W., S. Z., K. Z., P. Z., and X. S. made the substrates and investigated the scope. G. X. and T. C. supervised the project.

Competing interests

The authors declare no competing interests.

Additional information

Supplementary information The online version contains supplementary material available at https://doi.org/10.1038/s41467-024-50897-7.

Correspondence and requests for materials should be addressed to Tie-Gen Chen or Guoqin Xia.

Peer review information *Nature Communications* thanks Lingchao Cai, Sermadurai Selvakumar and the other anonymous reviewer(s) for their contribution to the peer review of this work. A peer review file is available.